Vcal Calibration Study of the Digital ROC

Kapustka, Brian

February 04, 2014

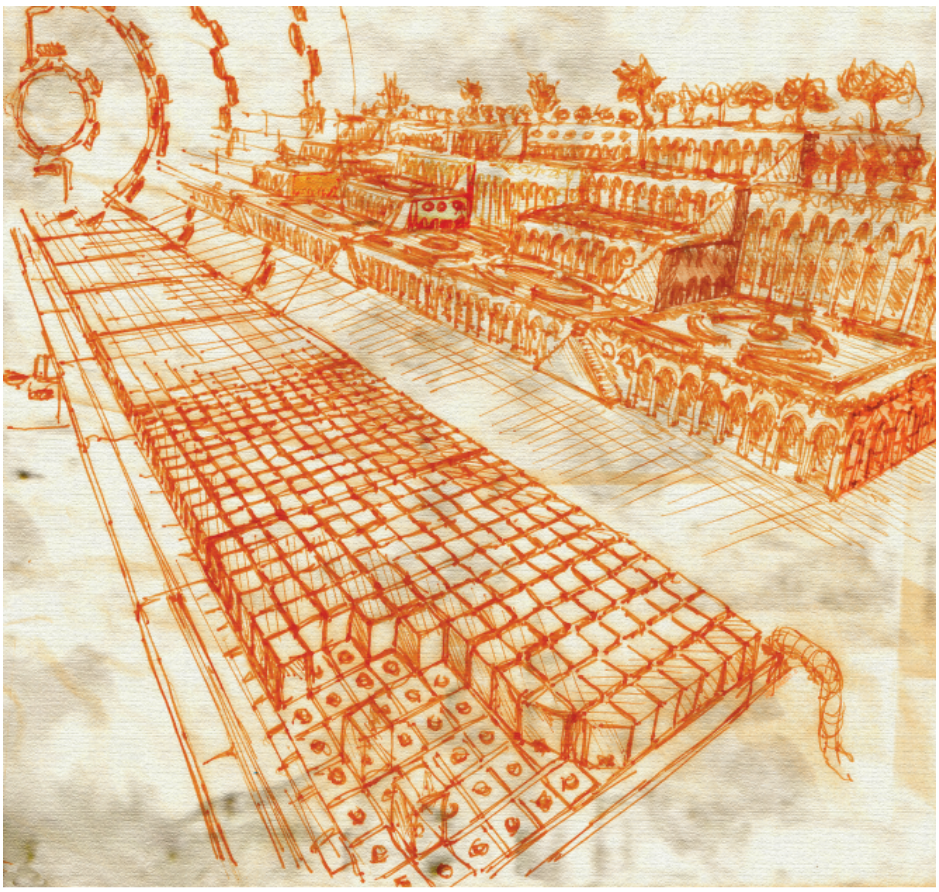

Abstract

The origional pixel detector was designed to operate with a luminosity of $1 \times 10^{34} cm^{-2} s^{-1}$, and a 25 ns bunch spacing, with close to 25 collisions per crossing. With the current upgrading of the accelerator, the luminosity and number of collisions per crossing will increase. An upgrade to the pixel detector is planned for the year 2018. These upgraded pixel detectors will exceed the design specifications of the current detector. However, there still remains much work to be done to understand, and characterize the proposed pixel detector.

Contents

1 Introduction

The Large Hadron Collider (LHC) began it's operation in 2010 with proton-proton collisions with a center of mass energy (CM) of 7TeV [1]. The CM energy for the entirety of 2012 was 8TeV. At the end of 2012 the cms experiment had seen a total intergrated luminosity of just over 29 fb^{-1}, as can be seen in Figure 1.

Early in 2013 the LHC went into the first of it's 3 larger shutdowns. These shut downs have been name LS1, LS2, and LS3. Currently, LS1 is due to end in January of 2015 [6]. During this time the CM energy will be increased to 14TeV. During the LS2, expected during 2018, the injector chain will be improved and upgraded. In LS3, expected during 2022, the LHC will have multiple upgrades to increase the size of bunch overlap.

The origional goal for LHC was to achieve an instantaneous luminosity of $1 \times 10^{34} cm^{-2} s^{-1}$[1]. It is expected that peak luminosities will reach close to $2 \times 10^{34} cm^{-2} s^{-1}$ before LS2. As a result, CMS must be prepared to handle the high pile-up ($\bar{PU}$) of 50 events per bunch crossing. The total intergrated luminosity is expected to reach an order of $200 fb^{-1}$ just before LS2, with $500 fb^{-1}$ achieved by LS3. The LHC also has a High Luminosity program (HL-HLC). This is expected to deliver a further $2500 fb^{-}$[1]. This will result in a $\bar{PU}$ of well over 100.

With higher CM energy and luminosity, leading to larger $\bar{PU}$, the CMS detector will need to undergo several upgrades to keep up. During LS1, the detectors are going through maintinence. During LS2 three major upgrades are planned: an upgrade to the pixel detector, improvements to the trigger L1 trigger system, and an upgrade to HCAL photo-electronics. The subject of this report will be centered on some of the testing done on the readout electronics that will be used for both the Pixel Detecter and its end caps.

2 The Pixel Detector

The current pixel detector is used for the first 3 layers of tracking in the Compact Muon Solenoid (CMS) detector. With a design luminosity of $1 \times 10^{34} cm^{-2} s^{-1}$, every cm^2 of the detector is hit with millions of particles per second when the LHC is running at peak luminosity[3]. The tracker, for this reason, which is closest to the beam pipe is limited by occupancy, and radiation damage. In order to manage these issues, it is neseccary to have

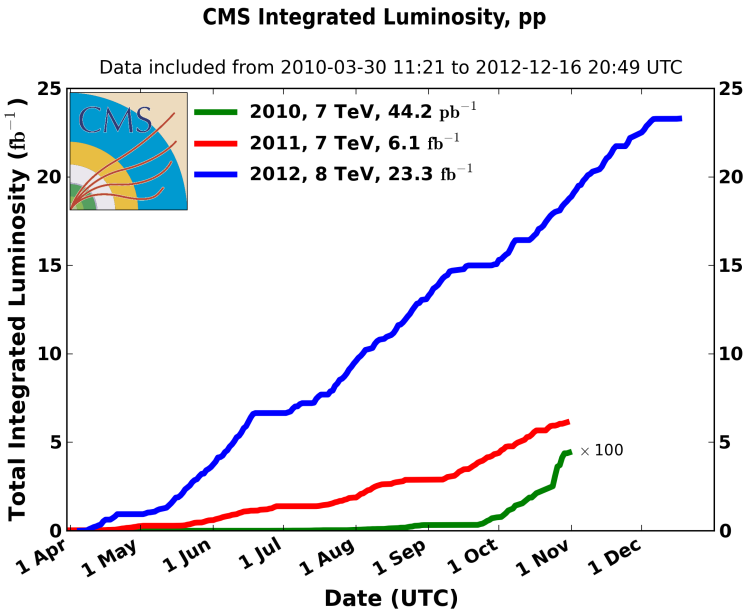

Figure 1: The multi-year intergrated luminosity plot for the years 2010 to 2012.

small sensors compared to microstrip detectors. This is why it is necessary to design a detecor around small strips, or pixels.

2.1 The Current Pixel Detector

The primary decision behind designing the pixel detector was to exploit the charge sharing caused by the the magnet that lies within the CMS detector. This magnet produces a magnetic field of 4 T. In Figure 2 is a depiction of how this effect would work. The resolution of the detector increases due to this charge sharing effect. A charged particle that deposits signal in only one pixel has a lower resolution than if it deposited charge in two pixels. If a particle deposits charge in more than 2 pixels then the data rate increases, the signal charge per pixel decreases, and resolution is not improved.

2.1.1 The Pixel

Due to the effect of charge sharing, the ideal size of a pixel is one in which a charged particle deposits signal charge in 2 pixels. With a pixel thickness of

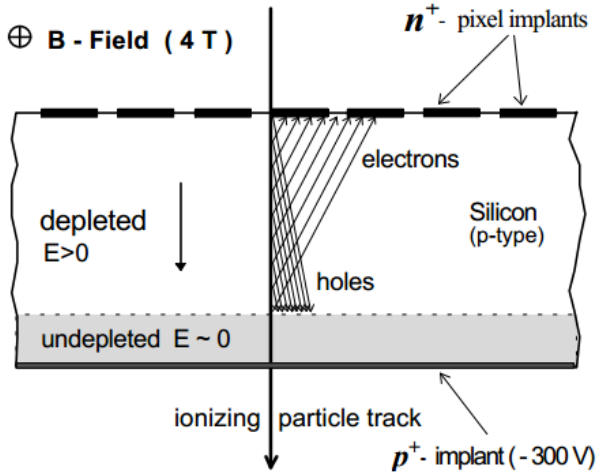

Figure 2: This is a figure of a charged particle traversing the pixel detector, the charge drift is caused by the 4 T magnetic field within the detector.

$\approx 300\mu m$, and a Lorentz angle of 28∘, this amounts to $\approx 150\mu m$. The actual pixel size, in the direction perpendicular to the magnetic field, is $100\mu m$ in order to maintain the effect of charge sharing[3]. The area of one pixel must be enpough to accommodate the readout electronics. This leads to the dimensions of $100\mu m \times 150\mu m$.

2.1.2 The ROC

A read out chip (ROC) is comprised of 4160 unit pixel cells (UPCs), 56 columns and 80 rows. It's purpose is to measure the amount of charge produced in the sensor, to amplify it, compare it to a threshold, and send out this threshold value with an address.

2.1.3 The Module

A module is comprised of 16 rocs, 2 rows by 8 columns. Additionally, it has a high density interconnect (HDI) which connects to the ROCs via wire bonds, as well as a token bit manager (TBM) chip on top. A TBM controls the readout and programming of a module. The tests discussed in this paper

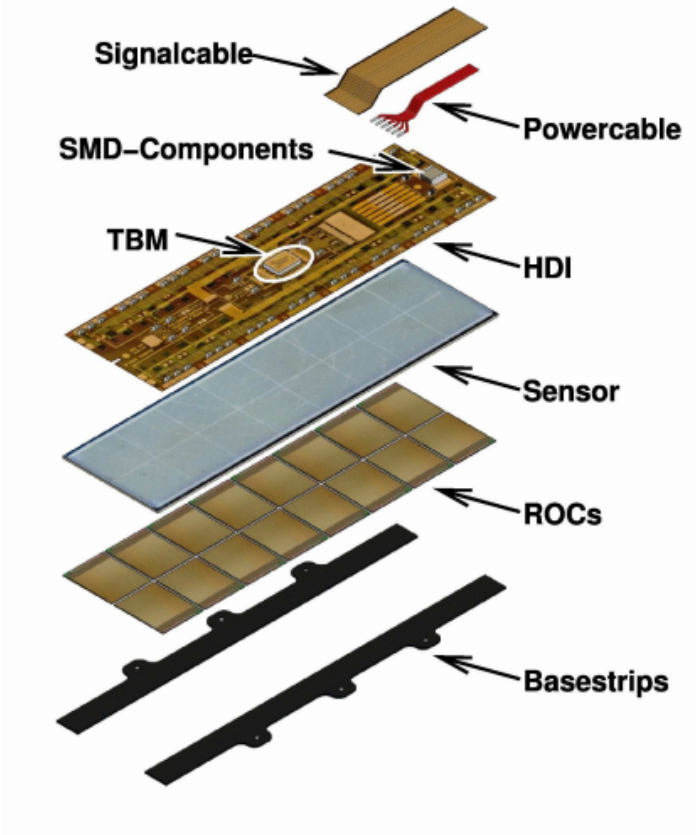

Figure 3: An image of a module, and how it is put together.

were done on individual ROCs, which have been adapted to be used outside of a module. An im age of what a module looks like can be found in Figure 3. The current module that are installed in the CMS detector are the *analog* version. They have an analog readout rate of 40 MHz.

2.2 The Digital ROC

Due to the increasing need to upgrade the current detector, which for now is operating at designed luminosity, a upgrade to the Module/ROC design is necessary. The problems faced by the old detector are:

- Data is lost due to higher occupancy, and trigger rate. This loss depends on both occupancy and trigger rates. These depend on buffer size and readout speed, respectivly.

- Lower tracking efficiency or higher fake rates at high pileup.
- Degredation in performance due to radiation damage[1]. Until recently, the detector has been running at designed luminosity, but not at designed temperature. This increase in temperature can cause large increases in the amount of radiation damage that the detector will sustain by a factor of double the damage per 7°C increase in temperature[5].
- Degradation in performance due to material. Currently the CMS pixel detector has 3 layers. The planned phase 2 upgrade will be adding a fourth layer. However, even with an extra layer the total material per volume will be less then it currently is. Less material, will lead to less undesired interactions betweeen particles and detector support materials.

The new ROC will take care of 3 of these issues by having: a faster digital readout, at 160 Mbits/s compared to 40 MHz analog; a time stamp buffer that is twice as large; a data buffer size that is more then doubled; a theoretical decrease in data loss by a factor of 2; and by containing less material[1].

3 Testing The Pixel Detector

As mentioned previously, a primary motivation of the pixel detector design was to exploit the effect of charge sharing that is caused by the magnetic field within the CMS detector. In order to do so, the pixel ROC has the ability to read out how much charge was deposited within a pixel in ADC units. This can then be converted into *Vcal* DAC units by using internal pulse height calibrations. This *Vcal* unit does not translate directly to energy, so in order to find the conversion from *Vcal* to energy, it is necessary to do calibration tests on each ROC. For this reason it is necessary to use x-ray photons, of a known energy, to deposit their charge via the photoelectric effect. A table listing the energies of these characteristic photons is shown in Table 1. An example of such a measurement can be seen in Figure 4.

3.1 Setup

For the tests that are discussed in this report, the setup is as follows:

Target	$E_{K_\alpha}(eV)$	N_{el}
Fe	6404	1779
Cu	8048	2236
Br	11924	3312
Mo	17479	4855
Ag	22162	6156
Sn	25044	6957
Ba	32193	8943

Table 1: This is a list of targets used in the energy calibrations of the ROC. The raw number of electrons is determined by the amount of energy required to release an electron. In slilcon. This is 3.6 eV, and so $N_{el} = E_{K_\alpha}/3.6eV$.

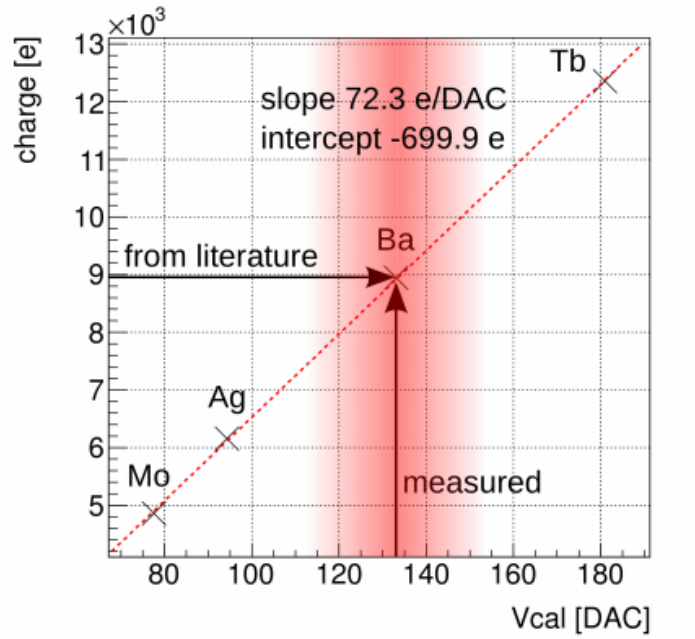

Figure 4: An example measurement showing the conversion of $Vcal$ to e^-.

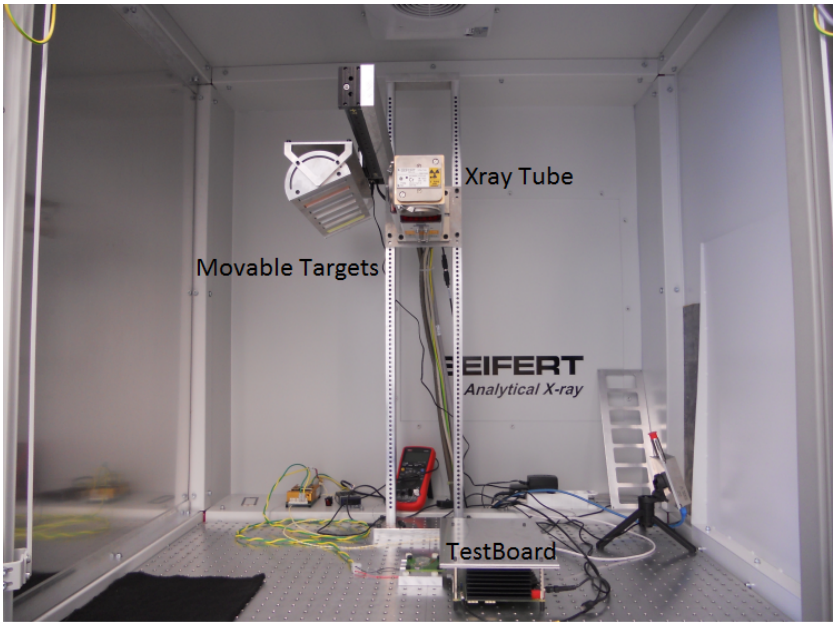

Figure 5: An image of the Xray Box used for the test setup.

- XrayBox, pictured in Figure 5, which contains:
  - XrayTube, for production of a continuous spectrum of X-rays
  - Movable array of fluorescence targets, with the targets mentioned in Table 1
  - A psi46 test board, for use with the ROCs being tested
- A single ROC cold box for a controlled environment in which to test the ROCs. It is used for managing the temperature and humidity of the test environment.
- software:
  - psi46expert, the software interface between a computer, and the testboard
  - elCommandante, a software framework which is planned to be used for the Phase 1 upgrade, it was used for automating the tests discussed in the following sections

3.2 The Pretest

Before taking data with a ROC, it is first required to run a pre-calibration test, reffered to as 'PreTest.' This test is always preformed when testing a new ROC as settings for each chip, or set of chips, can vary greatly from the last. A PreTest must also be preformed if the ROC(s) has(have) undergone large temerature changes. This test relies entirely on internal calibration signals, and so no irradiation is required[4].

3.3 Trimming

One of the more important pieces of each PUC is the comparator. It can compare charges that are injected or generated by a particle. These comparators have an adjustable threshold which is set globally for each ROC by the *VthrComp* DAC. When speaking about the *VthrComp* DAC it is important to note that lower values correspond to a higher threshold. The only input parameter to the trim algorithm is the theshold (in *Vcal* units), to which all pixels will be unified to. Other variables that go into consideration are the *Vtrim* DAC, and the trim bits for each individual pixel. The *Vtrim* DAC determines how much the trim bit value of each pixel lowers the threshold.

The trim bit test is carried out in the following manner:

- The first step is to find the value of *VthrComp* which correspons to the chosen threshold in *Vcal* units. This is done by measuring for each pizel its *VthrComp* threshold. Past this step, theshold can only be lowered, and so the minimum value of this distribution becomes the global *VthrComp* value.

- The second step of this test is to determine the appropriate *Vtrim* value. To find this the *Vcal* theshold is measured for all pixels. The pixel with the highest threshold is used to determine the necessary *Vtrim* value. For this pixel, the trim bits are set to 0. The value of the trim bits can range from 0 to 15. 0 lowers the threshold the most, while 15 doesnt lower the threshold at all.

- The final step is to successivly go through each pixel and determine the trim bit value which sets the threshold closest to the *Vcal* value. A before and after of the threshold distribution can be seen in Figure 6 [7].

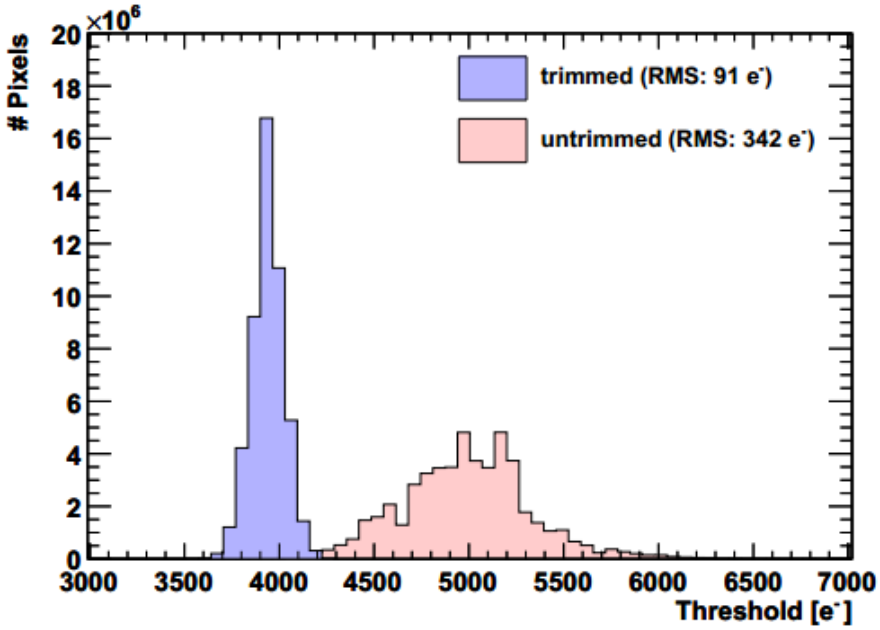

Figure 6: A comparison of theshold (in e^-) in a ROC before and after trimming.

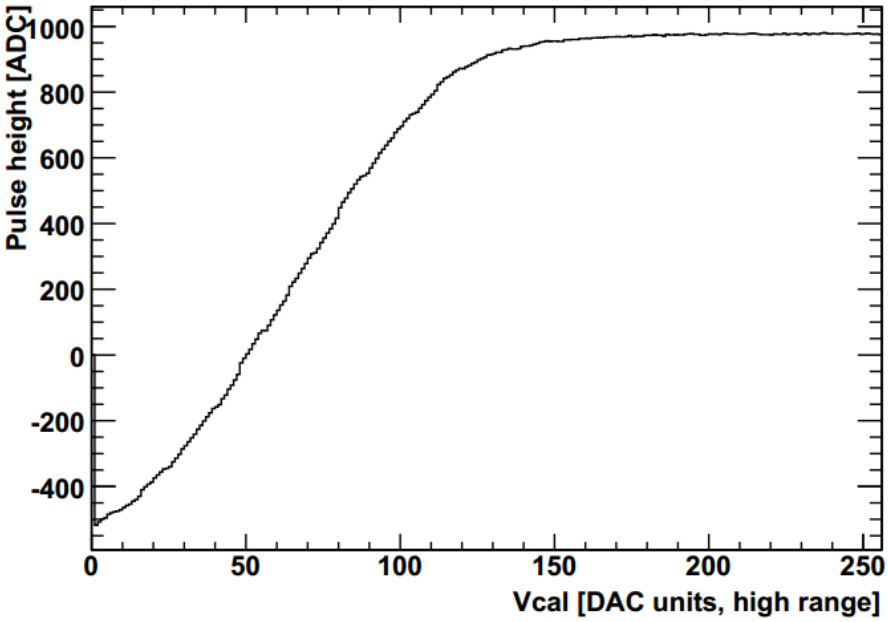

Figure 7: An example of a pulseheight calibration curve.

3.4 The PhCalibration Test

The pulse height calibration test is used to find the realationship between pulseheigh, measured in ADC units, and *Vcal* units. This is done by injecting a searies of increasing *Vcal* signals, and measuring the pulse height that results. This is done on a pixel by pixel basis, and an example of this can be seen in Figure 7 [2]. Ideally, this curve is linear for the range of *Vcal* units that are important, that is the lower range. This curve can be altered by changing the V_{sf} DAC. However, for the test results that are presented in this paper the V_{sf} DAC was not optimized.

3.5 The XraySpectrum Test

Using all the previous tests described, it is possible to run the XraySpectrum test. This method allows the ROC to take data for a specifed amount of time. After the time limit is reached, the ROC is read out through the testboard/psi46expert. Each pixel hit has an associated pulseheight (in ADC) associated with it. Thanks to the PhCalibration Test, this value can be con-

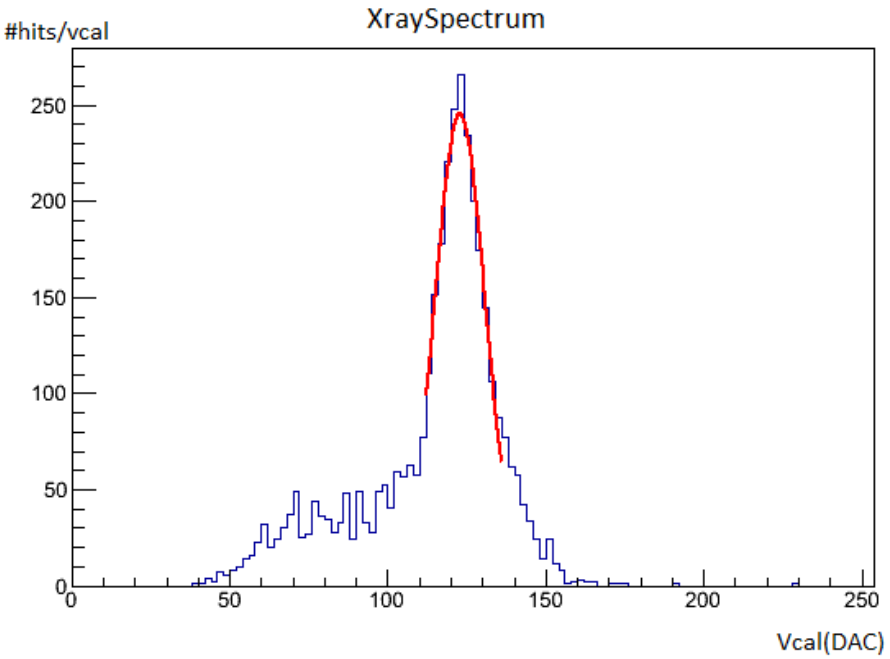

Figure 8: An example result from the XraySpectrum Test for a digital ROC.

verted to a *Vcal*. All of the *Vcal* values are histogramed. In the case that two pixels show a simultaneous hit, that particular hit is excluded from the analysis, as a significant portion of the energy is shared between the two. When using Xrays it is expected that a gausian distribution appears, while when observing radiation, a landau distribution appears[4]. For the distribution shown in Figure 8 a gausian is fit around the maximum, the "shoulder" is excluded. This procedure is also referred to as the *spectral method*.

3.6 The *VthrComp* Test

Using the parameters from the PreTest, and preferably a Trim test, it is possible to do a *VthrComp* test. This test is done by selecting a *VthrComp* value, and it results in the corresponding *Vcal* value. If this is done for a range of *VthrComp* values, then a conversion from *VthrComp* to *Vcal* can be attained. An example of this is shown in Figure 9.

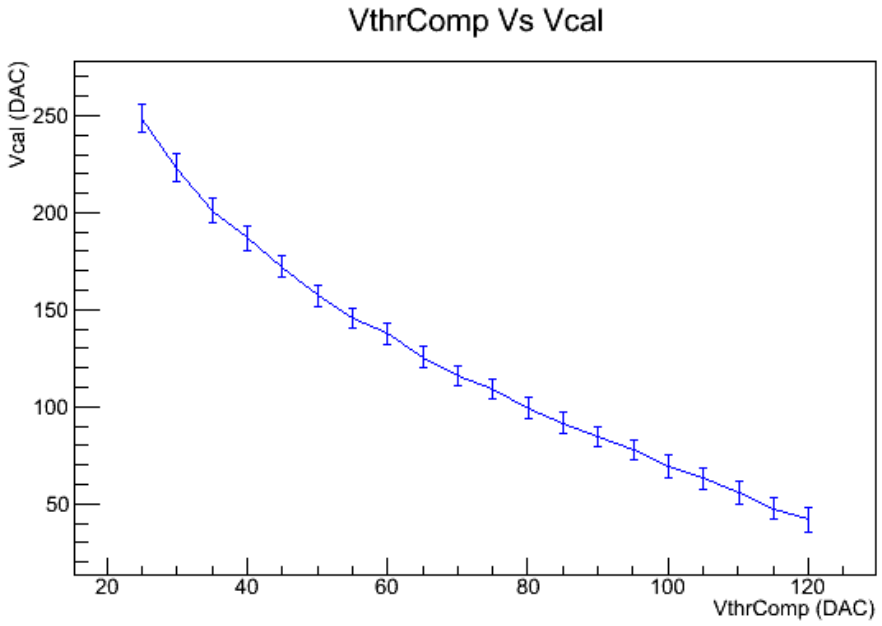

Figure 9: An example result of a series of *VthrComp* tests done on an analog ROC. For the Digital ROC this plot is linear.

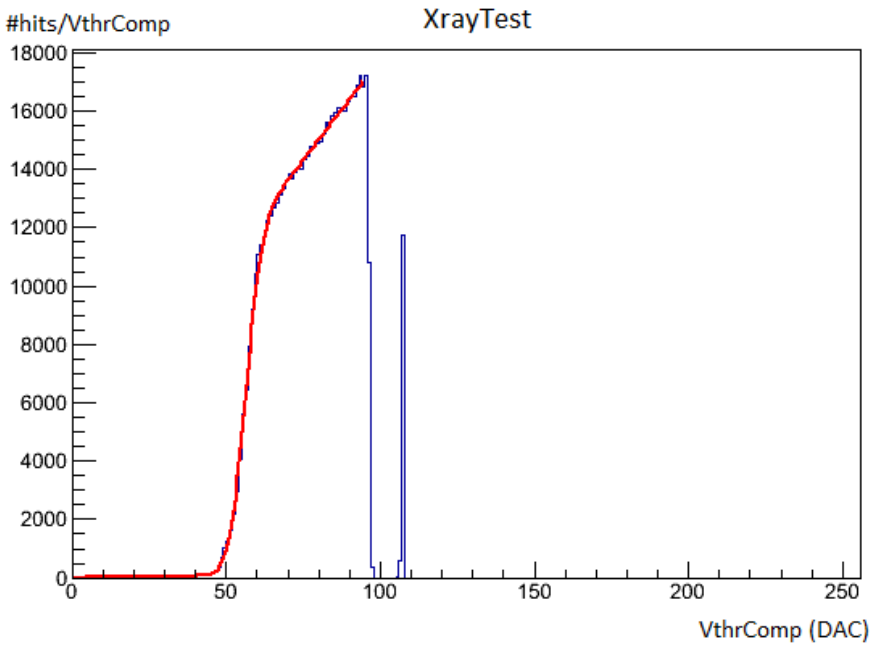

Figure 10: An example result from the XrayTest for an analog ROC.

3.7 The Xraytest

Using the parameters from the PreTest, and also preferably a Trim test, it is possible to do an Xray test. This is done by scanning a range of *VthrComp* values, and counting the number of hits. As the *VthrComp* DAC is scanned from lower to higher values, higher to lower thresholds respectivly, it is expected that at the energy of the Xrays that corresponds to the *VthrComp* threshold, there will be a half-way point for an S-curve. An example of this scan can be seen in Figure 10. In order to convert this *VthrComp* value, it is required to use the converstion for *VthrComp* to *Vcal* from the *VthrComp* test. This procedure is also referred to as the *threshold method*. In the following section the differences between the *spectral method* and the *threshold method* are discussed.

4 Results

The results presented in the following sections are comprised from several ROCs. There were 5 digital ROCs tested, as well as one analog ROC. These were tested at several temperatures varying between -20°C and 20°C in order to see if there is any termerature dependence of the amount of charge that each *Vcal* unit corresponds to.

4.1 XraySpectrum Test Results

The plots presented in Figures 11 and 12 are from the spectral method calibration measurements done on two ROCs; one analog and one digital, respectively. From these we can see that the digital ROC is not influenced by the temperature at which it is operating at when using the whole readout chain. However, the analog ROC does.

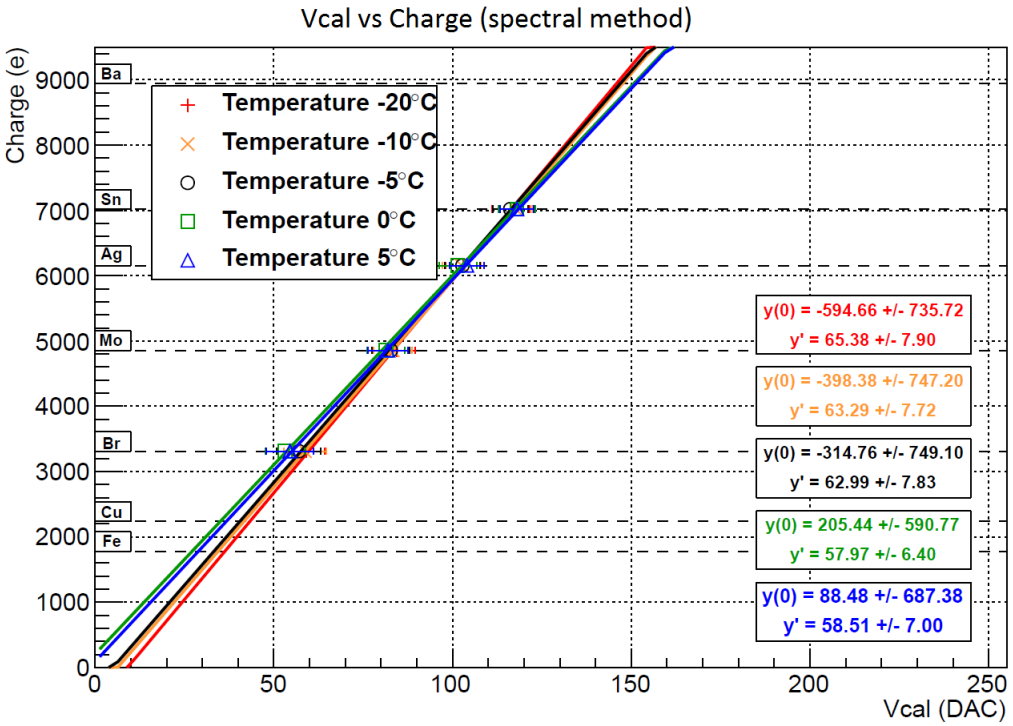

Figure 11: A spectral measurement done on an analog ROC across several temperatures.

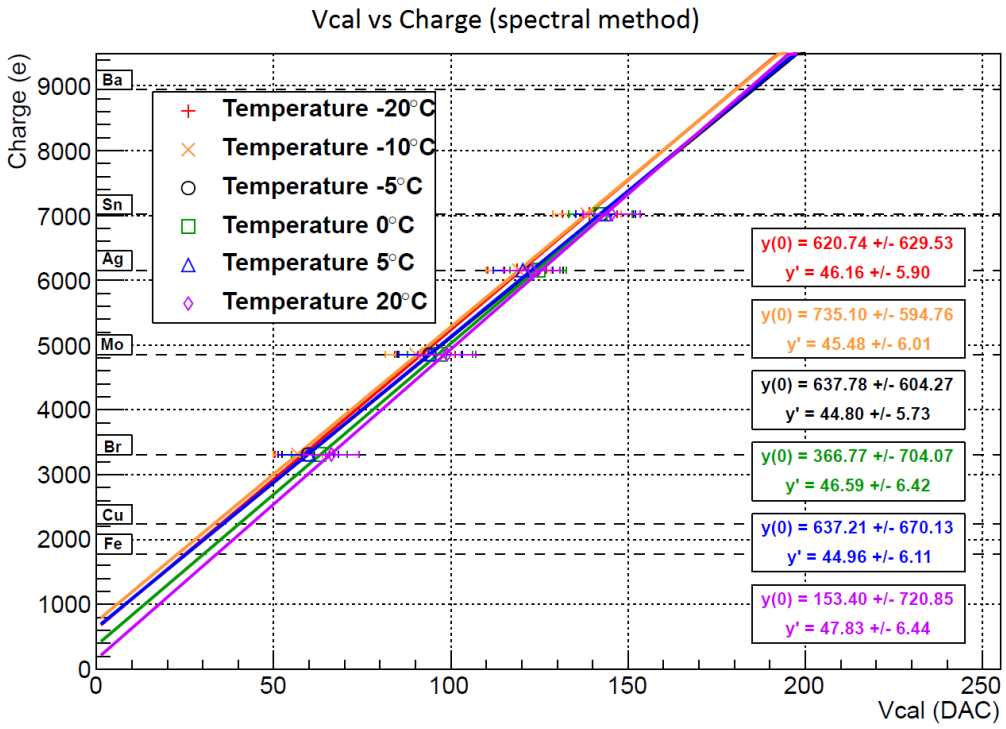

Figure 12: A spectral measurement done on a digital ROC across several temperatures.

4.2 Xraytest Results

The plots presented in Figures 13 and 14 are from the theshold method calibration measurements done,again, on two ROCs; one analog and one digital, respectively. From these it can be noted that the threshold method was only able to measure two characteristic Xrays for the digital ROC, when using just the comparator. Additionally, these two Xray energies are close to each other, and so the relative error for the slope is quite large. The reason for this is due to the fact that *VthrComp* now covers a smaller range of energies, with an overall lower threshold. By contrast, using the threshold method for the analog ROC, shows that this method is close to temerpature independent.

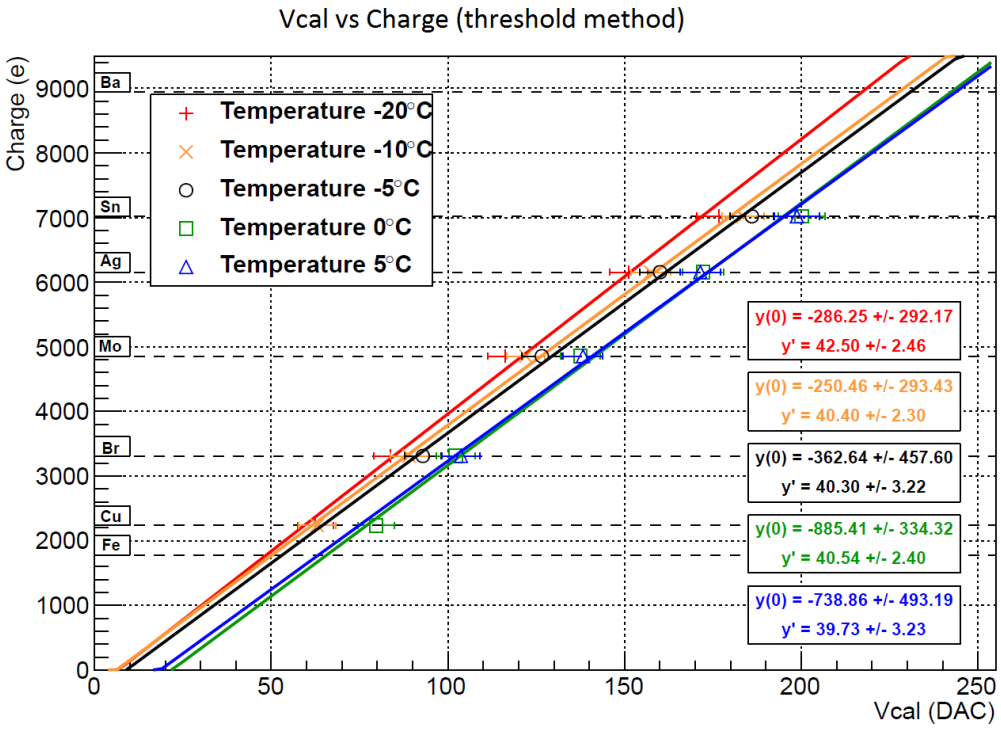

Figure 13: A threshold measurement done on an analog ROC across several temperatures.

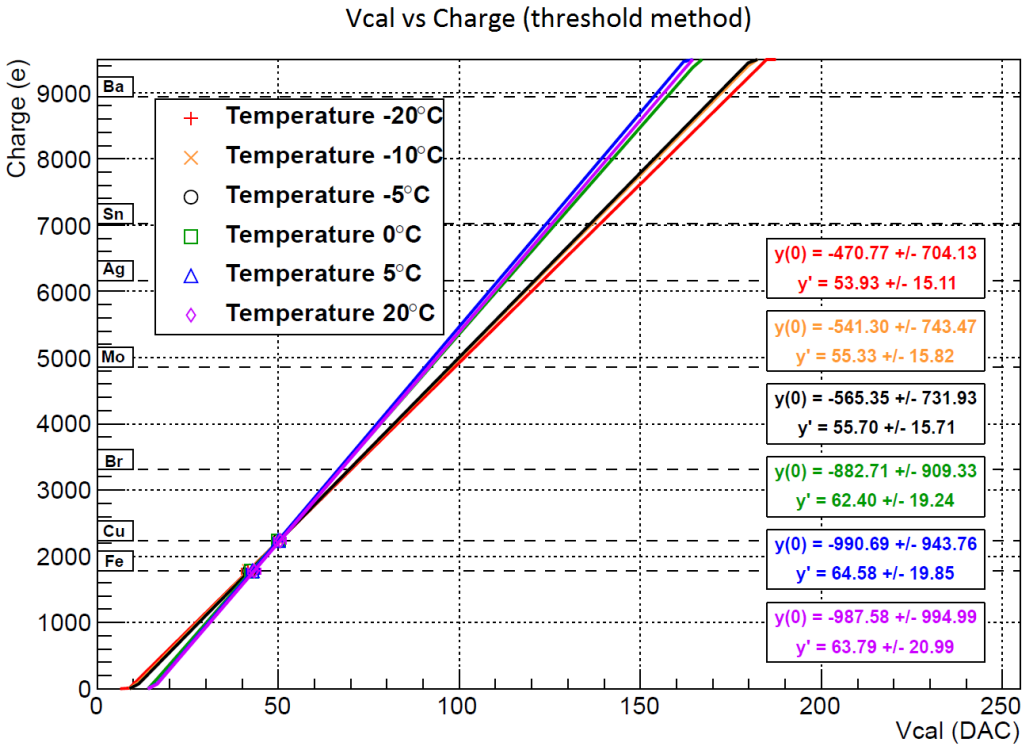

Figure 14: A threshold measurement done on a digital ROC across several temperatures.

4.3 Temperature Dependence Across Multiple ROCs

By extracting the slopes of each *Vcal* calibration, it is possible to show the temperature dependence by plotting the slope values against temperature. This is done in Figures 15 and 16 for both methods of calibration. Again, it is important to note that the threshold method is not a good one, when used on the digital ROC. By contrast, Figure 15 shows good results by the fact that the digital *Vcal* signal ROC does not appear to vary with temperature.

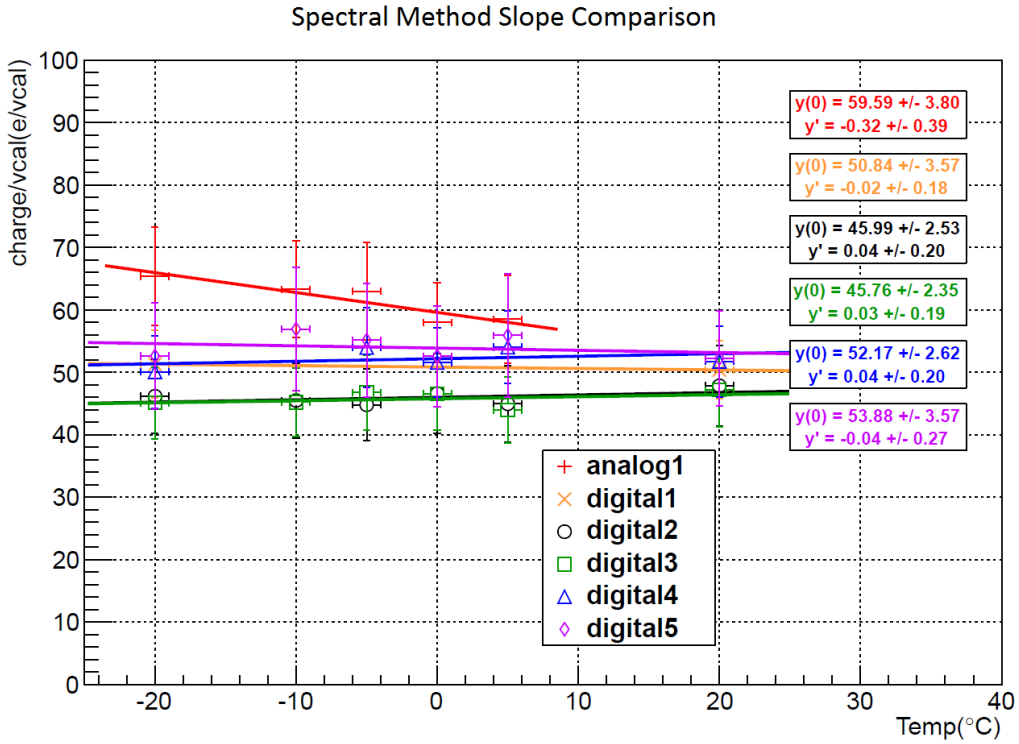

Figure 15: This plot shows the variation of e^-/Vcal with across several temperatures for all 6 ROCs when using the spectral method.

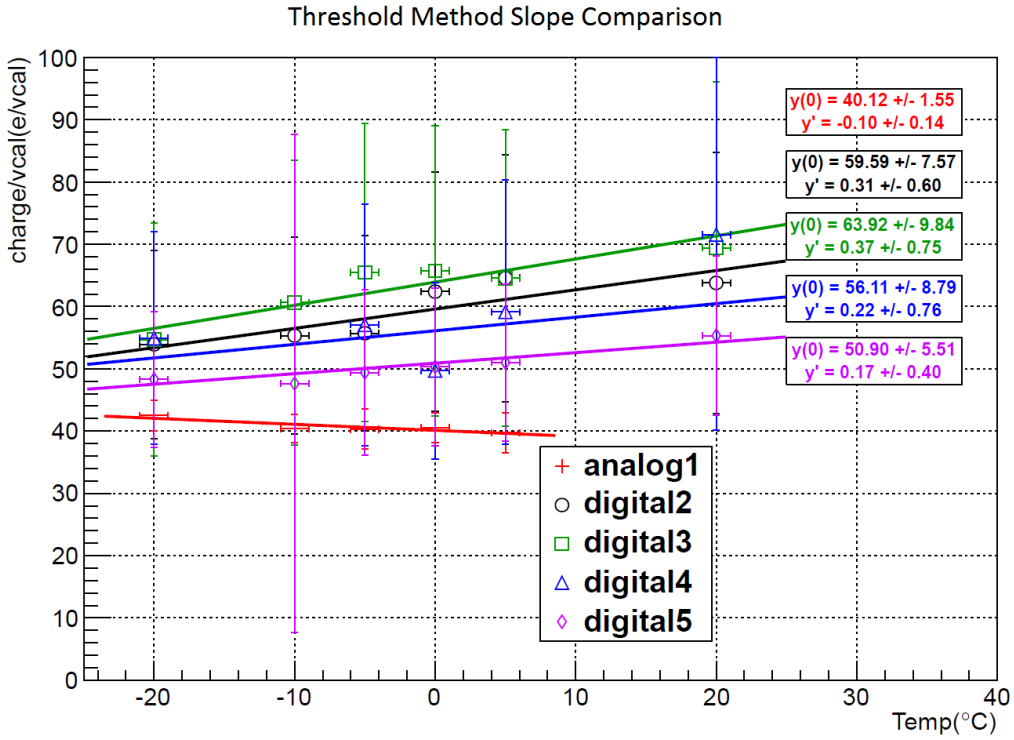

Figure 16: This plot shows the variation of e^-/Vcal with across several temperatures for all 6 ROCs when using the threshold method.

5 Conclusion

Following LS1, the LHC accelerator will reach almost double its previous CM energy, 13 TeV. The increas in luminosity associated with this will be double the design specification. An upgrade to the pixel detector will be necessary. Much testing has already begun with the goal of characterizing and understanding the components of the future detector. The measurements presented in the paper show that the energy calibrations of the Digital ROC are not temperature dependent, and this result will possibly have some bearing on how the Digital Modules will be calibrated and tested.

References

[1] Aaron Dominguez. CMS technical design report for the pixel detector upgrade, 2012.

[2] Sarah Dumbach. CMS pixel module readout optimization and study of the B^0 lifetime in the semieptonic decay mode., 2009. PhD Thesis, ETH Zurïch.

[3] Wolfram Erdmann. The cms pixel detector, May 2009.

[4] Jan Hendrik Hoβ. X-ray calibration of pixel detector modules for the phase 1 upgrade of the cms experiment., September 2012. Masters Thesis, Karlsruher Institut fär Technologie.

[5] Tilman Rohe, Peter Fischer, Leonardo Rossi, and Norbert Wermes. Pixel detectors: From fundamentals to applications.

[6] Anais Schaeffer. LS1 report: on the home straight in 2014, Dec 2013.

[7] Peter Trüb. CMS pixel module qualification and monte-carlo study of H $\rightarrow \tau^+\tau^- \rightarrow l^+l^- E_T^{miss}$, 2008. PhD Thesis, ETH Zurïch.